

Influence of redox processes on clay mineral transformation in Retisols in the Carpathian Foothills in Poland. Is a ferrollysis process present?

Wojciech Szymański¹ · Michał Skiba² · Artur Błachowski³

Received: 16 May 2016 / Accepted: 18 August 2016 / Published online: 9 September 2016
© The Author(s) 2016. This article is published with open access at Springerlink.com

Abstract

Purpose Ferrollysis is a soil-forming process, which involves destruction of clay minerals due to cyclic reduction and oxidation in acidic and periodically wet soils. The main objectives of this study were as follows: (1) to determine the influence of redox processes on clay mineral transformation in Retisols (Albeluvisols) in the Carpathian Foothills in Poland and (2) to verify the occurrence of ferrollysis in Retisols showing various degrees of bleaching.

Materials and methods Twelve representative soil profiles were selected for analysis. All were formed entirely from loess except for two profiles, in which the lowermost horizons (2C) had developed from weathered flysch rocks residuum. Soil mineral analysis was done using x-ray diffraction (XRD), Fourier-transform infrared (FTIR) spectroscopy, and Mössbauer spectroscopy (MS).

Results and discussion The obtained results indicate that the qualitative and quantitative mineral compositions of the clay fraction in the E and Eg horizons obtained from Retisols in the Carpathian Foothills exhibiting marked

differences in bleaching (strong, moderate, weak, and lack of bleaching) caused by periodic stagnation of water above a slowly permeable fragipan and cyclic redox processes are the same. The E and Eg horizons are characterized by the presence of 2:1 clay minerals with likely organic interlayer fillings, dioctahedral mica, kaolinite, and chlorite.

Conclusions The results indicate that (1) redox processes occurring in the soils do not affect clay mineral transformation in Retisols of the Carpathian Foothills in Poland and (2) ferrollysis is not the main soil-forming process operating in these soils. This is most likely because iron-bearing minerals are not abundant in the Retisols and/or undergo eluviation to the lower part of the soil profiles. The lower content of the clay fraction in the E and Eg horizons versus that in the lower soil horizons of the Retisols is related to clay illuviation (*lessivage*), and not to clay decomposition due to ferrollysis.

Keywords Carpathian Foothills · Clay minerals · Ferrollysis · Redox processes · Retisols · X-ray diffraction

Responsible editor: Dong-Mei Zhou

✉ Wojciech Szymański
w.szymanski@uj.edu.pl

¹ Institute of Geography and Spatial Management, Department of Pedology and Soil Geography, Jagiellonian University, ul. Gronostajowa 7, 30-387 Kraków, Poland

² Institute of Geological Sciences, Department of Mineralogy, Petrology and Geochemistry, Jagiellonian University, ul. Oleandry 2a, 30-063 Kraków, Poland

³ Institute of Physics, Department of Mössbauer Spectroscopy, Pedagogical University, ul. Podchorążych 2, 30-084 Kraków, Poland

1 Introduction

Soils with a contrasting texture are very common around the world (Kemp and McIntosh 1989; Phillips 2001, 2004, 2007; Świtoniak 2008, 2014; Świtoniak et al. 2016). According to the literature, such soils could be the result of different geologic and/or pedologic processes including sedimentation of different parent material (Phillips 2007; Świtoniak 2008, 2014; Świtoniak et al. 2016); clay eluviation-illuviation (Van Ranst and De Coninck 2002; Boivin et al. 2004; Świtoniak 2008, 2014; Świtoniak et al. 2016); bioturbation (Leigh 1998; Peacock and Fant

2002; Phillips 2007); and ferrollysis (Brinkman 1970, 1977, 1979; Brinkman et al. 1973).

Ferrollysis is a soil-forming process, which was first proposed by Brinkman (1970). It involves destruction of clay minerals due to cyclic reduction and oxidation in acidic and periodically wet soils (Brinkman 1970; Barbiero et al. 2010). Ferrollysis involves biochemical reduction of Fe^{3+} taking place during wet seasons and leading to mobilization of Fe and substitution of exchangeable cations within clay minerals with Fe^{2+} . During dry periods, Fe^{2+} oxidizes forming ferric hydroxides and protons which attacks structures of clay minerals. Thus, cyclic reduction and oxidation may cause decomposition of clay minerals leading to release of the lattice cations (e.g., Al, Mg, Fe). Except for the dissolution, soil clay minerals may undergo transformation due to the formation of Al- and/or Fe-hydroxy polymers within the interlayer space (Rich 1968; Brinkman 1970, 1977; Gerstl and Banin 1980). The transformation of 2:1 clay minerals due to the cyclic reduction and oxidation and formation of the clays with interlayer fillings is responsible for lowering their cation exchange capacity, mineral solubility, and swelling ability (Rich 1968; Brinkman 1979; Nakao et al. 2009; Szymański et al. 2014).

Ferrollysis is a common process in seasonally wet and acidic soils containing a hardly permeable horizon such as a plughpan (Brinkman 1977) and duripan (Hobson and Dahlgren 1998). Ferrollysis may also occur in soils with a fragipan. Fragipan shows low permeability which may lead to periodic water stagnation causing seasonal anaerobic conditions which favor reduction of iron oxides and their subsequent translocation and oxidation. Thus, it is very likely that ferrollysis may take place in Retisols containing a fragipan, because of the high bulk density and low porosity of the pan (e.g., Witty and Knox 1989; Lindbo et al. 1994; Ciolkosz et al. 1995; Szymański et al. 2011). The seasonal stagnation of water within Retisols causes the bleaching of soil material indicating reduction and dissolution of iron oxides and their subsequent re-oxidation and immobilization in the form of iron nodules, concretions, soft masses, and pore linings (Cescas et al. 1970; Schwertmann and Fanning 1976; Rhoton et al. 1993; Zhang and Karathanasis 1997; Lindbo et al. 2000; Dixon and White 2002; Szymański et al. 2011, 2012, 2014; Szymański and Skiba 2013). Similar changes in the valence of iron may occur within the structures of clay minerals containing iron in the octahedral sheet (e.g., Rich 1968; Brinkman 1977; Rozenson and Heller-Kallai 1978; Gerstl and Banin 1980; Hardy et al. 1999; Kohut and Warren 2002). However, Van Ranst and De Coninck (2002) as well as Van Ranst et al. (2011) have recently reported that ferrollysis does not take place in Retisols (previously called Albeluvisols) and soils exhibiting a stagnic

color pattern from Western Europe and in Planosols from Ethiopia.

Despite the fact that the redox processes are very common in various soils (Retisols, Stagnosols, Planosols, Gleysols, Fluvisols, paddy soils), very few is known about their impact on soil minerals and especially on clay minerals. In addition, very little studies present the results of qualitative and quantitative mineral composition of hydromorphic soils in the context of their genesis. Due to the above-mentioned contrasting results and reports concerning ferrollysis process in soil environment and still lacking of sufficient detailed mineralogical data from hydromorphic soils, we have decided to fill this gap.

The main objectives of this study were the following: (1) to determine the influence of redox processes on clay mineral transformation in Retisols (Albeluvisols) in the Carpathian Foothills in Poland and (2) to verify the occurrence of ferrollysis in Retisols showing various degrees of bleaching by means of qualitative and quantitative mineralogical analyses.

2 Materials and methods

2.1 Study area

The present study was carried out in the Carpathian Foothills in southern Poland (Fig. 1). The region is formed of a thick mantle of non-calcareous loess, which covers interbedded layers of sandstone, siltstone, and shale of turbiditic origin (i.e., Carpathian flysch). According to Klimaszewski (1967), the loess was transported on a short distance and accumulated during the last phase of glaciation (Vistulian) in the Pleistocene. The studied area is characterized by hilly relief with wide and flat hills showing elevation between 300 and 500 m a.s.l. (Starkel 1972). A moderately humid climate with mean annual air temperature between 6 and 8 °C and total annual precipitation from 700 to 900 mm (Hess 1965) as well as a lack of carbonates in the loess cover serve as the main reasons for the prevalence of Luvisols and Retisols (which until recently were called Albeluvisols) across the Carpathian Foothills (Skiba and Drewnik 2003; Szymański et al. 2011, 2012). The vegetation of the study area can be characterized by a mosaic of broadleaf forests (*Tilio-Carpinetum*) showing a prevalence of hornbeam (*Carpinus betulus* L.), lime (*Tilia cordata* Mill.), oak (*Quercus sessilis* Ehrh. and *Quercus robur* L.), and beech (*Fagus sylvatica* L.) as well as arable land, with potatoes (*Solanum tuberosum* L.), wheat (*Triticum aestivum* L.), and rye (*Secale cereale*) being the most popular crops. In some places, mixed forests (*Pino-Quercetum*) with oak (*Q. robur* L.) and pine (*Pinus silvestris* L.) are also present (Towpasz and Zemanek 1995).

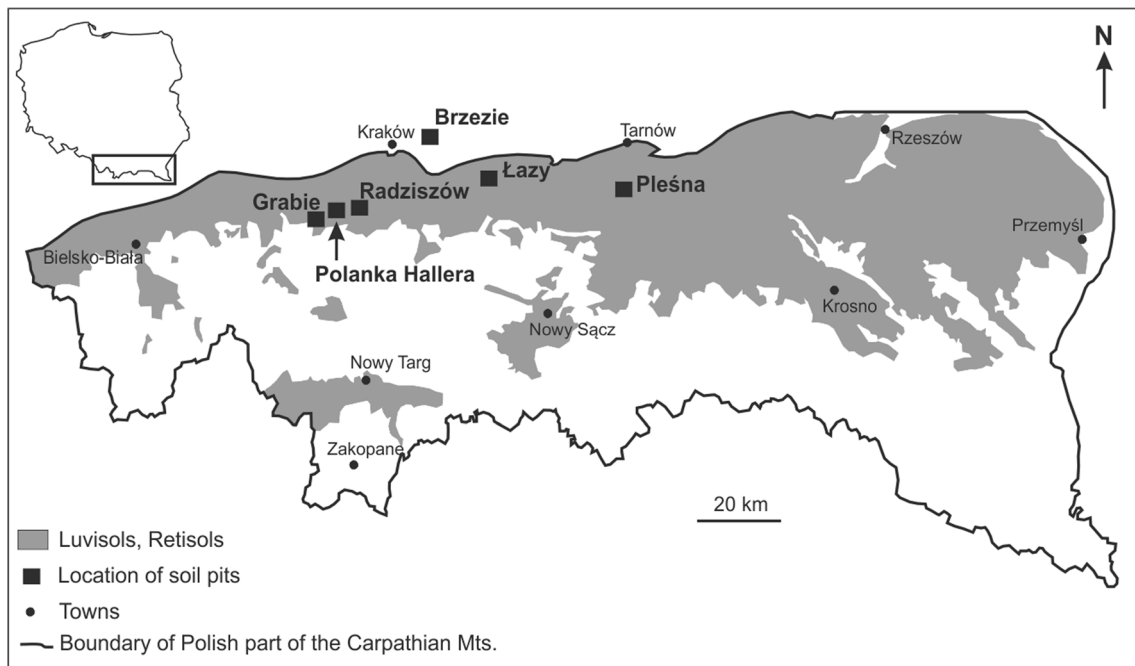


Fig. 1 Location of the soil profiles and occurrence of Luvisols and Retisols in the Polish part of the Carpathians (based on Skiba and Drewnik 2003)

2.2 Methods

Twelve representative soil profiles were selected for analysis. All were formed entirely from loess except for the Grabie and Radziszów profiles, in which the lowermost horizons (2C) had developed from weathered flysch rocks residuum. Figure 1 presents the geographic location of the soil profiles, while Table 1 summarizes detailed information about the study sites and classification of the soil profiles according to the World Reference Base for Soil Resources (WRB) system (IUSS Working Group WRB 2014).

During field studies, soil profiles were described and sampled. Soil samples were collected from each soil horizon in plastic bags and transported to the laboratory. In the laboratory, the samples were air dried, gently crushed, and sieved through a 2-mm sieve. All laboratory analyses were conducted on the fraction below 2 mm. Texture of soil material was determined by means of a set of sieves for the purpose of sand separation as well as the hydrometer method for silt and clay fractions (Gee and Bauder 1986). The content of organic carbon was determined using a rapid dichromate oxidation technique (Nelson and Sommers 1996), while pH was measured potentiometrically in distilled water using a 1:2.5 soil/water ratio (*w/v*) (Thomas 1996). Chemical composition of the fine-earth material (fraction <2 mm) was determined using inductively coupled plasma-emission spectrometry (ICP-ES) following digestion of the bulk samples with lithium metaborate/tetraborate and dilute nitric acid at Acme Labs (Vancouver, BC, Canada). Free forms of iron (Fe_d) extracted using dithionite-citrate-bicarbonate (DCB) were determined by means of atomic

absorption spectrometry (AAS) (Schlichting and Blume 1966). Amorphous forms of iron and aluminum (Fe_o , Al_o , respectively) were extracted with acid ammonium oxalate (Van Reeuwijk 2002) and determined using a spectrophotometer (Rayleigh UV-1601). The color of the soil material was described in the moist state using Munsell Color Soil Charts (where, e.g., 10YR means hue and 6/2 means value/chroma of color).

X-ray diffraction analyses were done using a Philips X'Pert diffractometer equipped with a PW3020 vertical goniometer, 1° divergence slit, 0.2 mm receiving slit, incident- and diffracted-beam Soller slits, 1° anti-scatter slit, graphite diffracted-beam monochromator, and a Cu x-ray lamp operated at 40 kV and 30 mA.

Quantitative analyses were performed on bulk soil samples (<2 mm) mixed with ZnO as internal standard using random powder mounts (Moore and Reynolds 1997). More details concerning the preparation of samples for quantitative analysis of the mineral composition can be found in Szymański et al. (2011) and Drewnik et al. (2014). Random specimens were scanned from 2 to $65^\circ 2\theta$ at a counting speed of $0.02^\circ/5$ s. To calculate the mineral composition of the bulk samples, the Seifert Rietveld AutoQuan/BGMN software was used (Taut et al. 1998). For calculation purposes, x-ray diffraction (XRD) data from $15^\circ 2\theta$ to $65^\circ 2\theta$ were used.

Clay fractions (<2 μm) were separated by centrifugation (using a centrifuge MPW-400) of 100 g bulk samples (<2 mm) dispersed in deionized water using an ultrasonic disintegrator. The centrifugation time was 3 min at the speed of 1000 rpm and the assumed density of particles was 2.65 Mg/m^3 (Jackson 1969). To obtain clay minerals in a natural state, the samples

Table 1 Detailed information about study sites and classification of the soils

Profile	Location	Geomorphology	Vegetation	Classification according to WRB (2014)
Pleśna 1	49° 56' 42" N; 20° 56' 51" E; 225 m a.s.l.	Gentle, concave, lower part of slope (<5°); exposure W	Tilio-Carpinetum	Dystric Glosic Fragic Retisol (Siltic, Cutanic, Densic)
Pleśna 2	49° 55' 10" N; 20° 56' 43" E; 255 m a.s.l.	Gentle, convex, upper part of slope (<5°); exposure NE	Crops	Dystric Glosic Fragic Retisol (Siltic, Cutanic, Densic)
Pleśna 3	49° 55' 20" N; 20° 56' 35" E; 236 m a.s.l.	Gentle, concave, lower part of slope (<3°); exposure NE	Crops	Dystric Albic Stagnic Glosic Fragic Retisol (Siltic, Cutanic, Densic)
Pleśna 4	49° 55' 50" N; 20° 57' 50" E; 345 m a.s.l.	Almost flat summit of hill (<2°); exposure NW	Tilio-Carpinetum	Dystric Stagnic Glosic Fragic Retisol (Siltic, Cutanic, Densic)
Łazy 1	49° 58' 03" N; 20° 29' 25" E; 255 m a.s.l.	Gentle, convex, middle part of slope (<5°); exposure S	Crops	Stagnic Glosic Fragic Retisol (Siltic, Cutanic, Densic)
Łazy 2	49° 58' 15" N; 20° 29' 05" E; 260 m a.s.l.	Gentle, convex, upper part of slope (<5°); exposure NW	Pino-Quercetum	Dystric Stagnic Glosic Fragic Retisol (Siltic, Cutanic, Densic)
Łazy 3	49° 57' 95" N; 20° 29' 71" E; 245 m a.s.l.	Gentle, convex, upper part of slope (<5°); exposure N	Meadow	Stagnic Glosic Fragic Retisol (Siltic, Cutanic, Densic)
Łazy 4	49° 57' 59" N; 20° 29' 07" E; 280 m a.s.l.	Flat summit of hill (0°)	Pino-Quercetum	Dystric Stagnic Glosic Fragic Retisol (Siltic, Cutanic, Densic)
Grabie	49° 54' 57" N; 19° 44' 53" E; 329 m a.s.l.	Almost flat summit of hill (<2°); exposure S	Pino-Quercetum	Dystric Stagnic Glosic Fragic Retisol (Siltic, Cutanic, Densic)
Radziszów	49° 55' 10" N; 19° 50' 08" E; 315 m a.s.l.	Almost flat summit of hill (<2°); exposure SE	Pino-Quercetum	Dystric Albic Stagnic Glosic Fragic Retisol (Siltic, Cutanic, Densic)
Polanka Hallera	49° 56' 00" N; 19° 45' 35" E; 310 m a.s.l.	Almost flat summit of hill (<3°); exposure SE	Crops	Eutric Albic Stagnic Glosic Fragic Retisol (Siltic, Cutanic, Densic)
Brzezie	50° 00' 15" N; 20° 10' 70" E; 210 m a.s.l.	Footslope (<2°); exposure N	Crops	Dystric Albic Stagnic Glosic Fragic Retisol (Siltic, Cutanic, Densic)

were separated without any chemical pretreatment. Oriented mounts with a surface density of 10 mg/cm² were prepared from the separated clay fractions by means of a glass slide technique (Środoń, 2006). XRD patterns for the oriented specimens were registered in air dry state, after heating for 1 h at 330 and at 550 °C, and after solvation, the mounts with liquid glycerol. The identification of clay minerals was performed according to operational definitions given by Środoń (2006). Analyses of XRD patterns were conducted by means of a ClayLab software (Mystkowski 1999).

Fourier-transform infrared (FTIR) spectra for the clay fractions were collected for random powder specimens dispersed in KBr pellets using a Bio-Rad FTS 135 FTIR spectrometer. The pellets (1.6 mg sample/300 mg KBr) were prepared from the natural clay fraction (<2 µm) that was previously dried by heating at 105 °C for 24 h and from KBr powder that was preheated at 550 °C for 24 h. Following the collection of the FTIR spectra, the pellets were heated at 180 °C for 12 h, and after cooling in a desiccator, analyzed again. Thirty-two scans were collected for each sample in the range from 400 to 4000 cm⁻¹ with a resolution of 2 cm⁻¹. The FTIR spectra were processed using a Spekwin32 software.

Mössbauer spectroscopy measurements were performed at room temperature using a RENON MsAa-3 spectrometer equipped with an LND Kr-filled proportional detector and He–Ne laser-based interferometer used to calibrate a velocity scale. A commercial ⁵⁷Co(Rh) source was applied for the 14.41-keV resonant transition in ⁵⁷Fe. The absorber for Mössbauer measurements was prepared in powder form and the thickness of the absorber was 90 mg/cm² of the investigated material. Data were fitted following the transmission integral approach using the MOSGRAF software suite.

Differences in mineralogical composition were evaluated by *t* Student test (level of significance at *p* < 0.05). All statistical calculations were done using Statistica 12 software.

3 Results and discussion

3.1 Morphology, physical, and chemical properties

The morphologic description of the soil profiles is summarized in Table 2. All the soil profiles show similar morphology, i.e., A-E-Btx-Btg-BC-C. The two main differences between the soils are the occurrence of organic horizons (O) in forest soils and strong (Pleśna 3, Pleśna 4, Łazy 1, Polanka Hallera, and Brzezie profiles); moderate (Łazy 3, Łazy 4, Grabie, and Radziszów profiles); or very weak or even nonexistent (Pleśna 1, Pleśna 2, and Łazy 2 profiles) bleaching of the eluvial part of the profile. The bleaching classification was done according to Munsell soil color charts in moist state: 10YR 6/2; 10YR 7/2–8/2, 2.5Y 6/2 (strongly bleached soil horizons); 10YR 4/3–5/3 (moderately bleached soil horizons); and

10YR 5/4 (very weakly or not bleached soil horizons). In addition, Pleśna 4, Łazy 4, and Radziszów profiles were further characterized by a bipartite eluvial horizon with an upper part showing lack of bleaching and a lower part (along the contact with the lower illuvial horizon) exhibiting moderate or strong bleaching. Topsoil horizons show black or brownish color, lack of Fe–Mn nodules and clay coatings on ped faces. Eluvial horizons (AE, E, Eg) exhibit more pale and/or bleached color and occurrence of hard Fe–Mn nodules. However, the Eg horizons contain more Fe–Mn nodules than the E horizons based on visual inspection of the soil profiles (Table 2). The lower part of the soil profiles usually exhibits mottled color. Additionally, the lower soil horizons are characterized by presence of many hard and soft Fe–Mn nodules, and many clay coatings on ped faces and clay infillings in channels (Table 2) (Szymański et al. 2011, 2012). Such a morphology of the soils is very typical for Retisols (Albeluvisols) occurring in different areas around the world (e.g., Brinkman 1979; Lindbo et al. 1994, 1995, 2000; Montagne et al. 2008; Kalinina et al. 2013; Sauer et al. 2013; Nikorych et al. 2014).

All the soils show a silt loam texture with a predominance of the silt fraction (Table 3). The topsoil and eluvial horizons contain markedly lower amounts of the clay fraction in comparison with lower horizons. Such a distribution of the clay fraction and the presence of many clay coatings and clay infillings clearly indicate a vertical translocation of the clay fraction in the soil profiles (Zasoński 1983, 1992; Lindbo and Veneman 1993; Weisenborn and Schaetzl 2005; Szymański et al. 2011, 2012). The lower part of the soil is characterized by higher bulk density and lower total porosity than those of the upper soil horizons (Table 3). The lower bulk density and higher total porosity of the upper soil horizons relative to lower soil horizons also indicate depletion of the finest particles and their accumulation in the lower part of the soils (Szymański et al. 2011, 2012, 2014; Nikorych et al. 2014).

The majority of the soils exhibit acidic or slightly acidic pH and only the Polanka Hallera profile is characterized by a slightly alkaline pH in some soil horizons, which is due to the liming.

Soil organic carbon (SOC) is concentrated mainly in topsoil horizons and its content in the horizons of forest soils ranges from 1.2 % to 6.1 % and is markedly higher than SOC content in topsoil horizons of arable soils (0.7 % to 1.2 %). Eluvial and illuvial soil horizons contain a very low amount of SOC (0.1 % to 0.7 %) (Table 3).

The content of DCB-extractable iron (Fe_d) and AAO-extractable iron and aluminum (Fe_o and Al_o, respectively) is shown in Table 3. Fe_d content is lower (statistically significant at *p* < 0.05) in topsoil and eluvial horizons (3.73 to 9.02 g kg⁻¹ with a mean of 5.22 g kg⁻¹) than in lower horizons (Btx, Btg, BC, C) (4.35 to 17.83 g kg⁻¹ with a mean of 7.87 g kg⁻¹), indicating translocation of Fe_d with clay minerals down the

Table 2 Field description of morphology of the soils

Horizon	Depth (cm)	Color (moist)	Structure	Consistence	Roots	Fe–Mn nodules	Clay coatings
Plešna 1							
O	0–2	N.A.	N.A.	N.A.	N.A.	N.A.	N.A.
A	2–10	10YR 4/2	sub- to angular blocky	soft	+++	absence	absence
AE	10–30	10YR 5/3	sub- to angular blocky	soft	++	few	absence
E	30–70	10YR 5/4	sub- to angular blocky	slightly hard	+	absence	absence
Btx	70–105	10YR 4/6	prismatic	very hard	few	+++	+++
Btg	105–150	10YR 4/6	prismatic	very hard	absence	absence	+++
BC	150–200	10YR 5/4	massive	hard	absence	absence	absence
Plešna 2							
A	0–10	10YR 5/3	subangular blocky	slightly hard	+++	absence	absence
AE	10–30	10YR 5/4	sub- to angular blocky	slightly hard	++	absence	absence
E	30–55	10YR 5/4	sub- to angular blocky	slightly hard	+	few	absence
Btx1	55–80	10YR 5/6; 10YR 6/4	prismatic	hard	few	+++	+++
Btx2	80–160	10YR 5/6; 10YR 6/4	prismatic	very hard	absence	+++	+++
Plešna 3							
Ap	0–35	10YR 4/3	angular blocky	slightly hard	+++	absence	absence
Eg	35–45	10YR 6/2	angular blocky	slightly hard	+	+++	absence
Btx1	45–100	10YR 5/4; 10YR 6/2	prismatic	very hard	few	+++	+++
Btx2	100–180	10YR 5/3; 10YR 6/2	prismatic	very hard	absence	+++	+++
Btg	180–245	10YR 5/2; 10YR 6/2	massive	hard	absence	+	+
BCg	245–285	10YR 5/2	massive	hard	absence	+	+
Plešna 4							
O	0–2	N.A.	N.A.	N.A.	N.A.	N.A.	N.A.
A	2–10	10YR 2/1	sub- to angular blocky	soft	+++	absence	absence
E	10–40	10YR 5/4	sub- to angular blocky	slightly hard	+++	absence	absence
Eg	40–90	2.5Y 6/2	angular blocky	hard	few	+++	absence
Btx	90–150	10YR 4/6; 2.5Y 6/2	prismatic	very hard	absence	++	+++
Lazy 1							
Ap	0–35	10YR 3/3	subangular blocky	soft	+++	absence	absence
Eg	35–50	10YR 6/2	ang- to subangular blocky	slightly hard	+	+	absence
Btx	50–70	10YR 5/6; 10YR 8/1	angular blocky	slightly hard	few	+++	+++
Btg	70–90	10YR 5/6	angular blocky	hard	absence	absence	+++
BC	90–110	10YR 5/4	ang- to subangular blocky	hard	absence	absence	+
C	110–150	10YR 5/4	massive	hard	absence	absence	absence
Lazy 2							
Ol	0–5	N.A.	N.A.	N.A.	N.A.	N.A.	N.A.
Of	5–8	N.A.	N.A.	N.A.	N.A.	N.A.	N.A.
A	8–20	10YR 3/2	sub- to angular blocky	soft	+++	absence	absence
E	20–55	10YR 5/4	subangular blocky	slightly hard	++	absence	absence
Btx1	55–65	10YR 4/6	angular blocky	hard	few	few	+++
Btx2	65–85	10YR 4/6	angular blocky	very hard	few	few	+++
Bt	85–115	10YR 4/6	angular blocky	very hard	few	few	+++
BC	115–135	10YR 4/6	angular blocky	very hard	few	absence	++
C	135–185	10YR 4/6	massive	very hard	absence	absence	absence
Lazy 3							
Ol	0–3	N.A.	N.A.	N.A.	N.A.	N.A.	N.A.
A	3–11	10YR 3/3	sub- to angular blocky	soft	++	absence	absence
AE	11–25	10YR 4/3	sub- to angular blocky	soft	+	absence	absence
Eg	25–50	10YR 4/3	sub- to angular blocky	soft	few	few	absence
Bh	50–70	10YR 3/3; 10YR 2/3	sub- to angular blocky	slightly hard	few	absence	+
Btx1	70–110	10YR 4/6; 10YR 6/4	prismatic	very hard	few	+++	+++
Btx2	110–160	10YR 5/6; 10YR 6/4	prismatic	very hard	absence	+++	+++
Lazy 4							
Ol	0–2	N.A.	N.A.	N.A.	N.A.	N.A.	N.A.
Ah	2–5	10YR 2/2	subangular blocky to granular	soft	+++	absence	absence
E	5–20	10YR 5/4	angular blocky	slightly hard	++	few	absence
Eg	20–35	10YR 5/3	angular blocky	slightly hard	+	++	absence
Btx1	35–60	10YR 5/4; 10YR 6/2	prismatic	very hard	few	+++	+++
Btx2	60–85	10YR 5/6; 10YR 6/2	prismatic	very hard	few	+++	+++
Btg	85–140	10YR 5/4; 10YR 5/6	prismatic	very hard	absence	++	++
BCg	140–180	10YR 5/4; 10YR 5/6	massive	hard	absence	++	+
Grabie							
Ol	0–2	N.A.	N.A.	N.A.	N.A.	N.A.	N.A.
Ofh	2–4	N.A.	N.A.	N.A.	N.A.	N.A.	N.A.
Ah	4–12	10YR 2/2	subangular blocky to granular	soft	+++	absence	absence

Table 2 (continued)

Horizon	Depth (cm)	Color (moist)	Structure	Consistence	Roots	Fe–Mn nodules	Clay coatings
Eg	12–35	10YR 5/3	ang- to subangular blocky	slightly hard	++	++	absence
Btx1	35–70	10YR 4/6; 10YR 6/4	prismatic	very hard	few	+++	+++
Btx2	70–120	10YR 5/6; 10YR 6/4	prismatic	very hard	few	++	+++
Btx3	120–155	10YR 5/6; 10YR 7/1	prismatic	very hard	few	++	++
2C	155–165	2.5Y 5/4	massive	very hard	few	absence	absence
Radziszów							
Of	0–2	N.A.	N.A.	N.A.	N.A.	N.A.	N.A.
Ah	2–12	10YR 2/2	granular to subangular blocky	soft	+++	absence	absence
E	12–35	10YR 5/4	ang- to subangular blocky	slightly hard	++	few	absence
Eg	35–45	10YR 5/3	ang- to subangular blocky	slightly hard	+	++	absence
Btx1	45–75	10YR 5/6; 10YR 7/2	prismatic	very hard	few	++	+++
Btx2	75–100	10YR 5/6; 10YR 7/2	prismatic	very hard	few	+++	+++
Btx3	100–120	10YR 5/6; 2.5Y 6/2	prismatic	very hard	few	++	+
BC	120–130	10YR 5/6; 2.5Y 6/2	massive	very hard	few	++	+
2C	130–160	2.5Y 5/4	massive	very hard	absence	absence	absence
Polanka Hallera							
Ap	0–20	10YR 3/3	subangular blocky	slightly hard	+	absence	absence
A	20–37	10YR 3/3	sub- to angular blocky	hard	+	absence	absence
Eg	37–50	10YR 8/2	subangular blocky	hard	absence	+++	absence
Btx	50–60	10YR 5/4; 10YR 8/2	prismatic	very hard	absence	++	+++
Btg1	60–85	10YR 5/4; 10YR 8/2	prismatic	very hard	absence	++	+++
Btg2	85–120	10YR 5/4; 10YR 8/2	prismatic	very hard	absence	++	+++
Btg3	120–155	10YR 5/8; 10YR 7/3	prismatic	very hard	absence	+	+++
Btg4	155–180	10YR 6/6; 2.5Y 7/2	prismatic	very hard	absence	+	++
Brzezie							
Ap	0–25	10YR 5/3	angular blocky	slightly hard	+++	absence	absence
AE1	25–40	10YR 5/4	angular blocky	slightly hard	++	absence	absence
AE2	40–58	10YR 5/3	angular blocky to granular	slightly hard	++	absence	absence
Eg	58–70	10YR 7/2	angular blocky to granular	slightly hard	+	+++	absence
Btx	70–95	10YR 6/8; 10YR 7/2	prismatic	hard	few	+++	+++
Btg1	95–115	10YR 6/6; 10YR 6/1	prismatic	hard	absence	+++	+++
Btg2	115–180	10YR 6/6; 10YR 7/1	prismatic	hard	absence	++	+++

N.A. not analyzed

soil profile. Bleached eluvial soil horizons (Eg) exhibit a slightly higher (but not statistically significant at $p < 0.05$) mean content of Fe_d (5.33 g kg^{-1}) than other eluvial horizons (E), in which the mean content of Fe_d is 4.81 g kg^{-1} . Fe_o and Al_o content is slightly higher in A, AE, E, and Eg horizons (with a mean of 2.62 and 0.92 g kg^{-1} , respectively) than in lower soil horizons (with a mean of 2.13 and 0.85 g kg^{-1} , respectively) or is evenly distributed throughout the soil profiles (Table 3). Mean Fe_o content is only slightly higher (but not statistically significant at $p < 0.05$) in E horizons (2.57 g kg^{-1}) than in Eg horizons (2.49 g kg^{-1}), while mean Al_o content is only slightly lower (but statistically significant at $p < 0.05$) in E horizons (0.82 g kg^{-1}) than in Eg horizons (0.98 g kg^{-1}).

The soil material collected from the soil profiles ($<2 \text{ mm}$) is composed mainly of SiO_2 , Al_2O_3 , Fe_2O_3 , and K_2O . The content of other compounds (CaO, MgO, Na_2O , TiO_2 , P_2O_5 , and MnO) in almost all of the soils is below 1 % (Table 4). Upper soil horizons (A, AE, E, and Eg) contain a higher amount of SiO_2 and a lower amount of Al_2O_3 , Fe_2O_3 , K_2O , CaO, and MgO in comparison with the lower part (Btx, Btg, BC, C) of the soils. However, slightly higher amount of MgO and CaO

in surface horizons of some soils (e.g., Pleśna 2, Łazy 3, and Łazy 4) relative to the eluvial horizons is most likely caused by “biocycling.” It should be noted that differences in the chemical composition of the E and Eg horizons are negligible (Table 4).

3.2 Mineral composition of the eluvial horizons

3.2.1 X-ray diffraction

The mineral composition of the clay fractions ($<2 \text{ }\mu\text{m}$) separated from the eluvial soil horizons showing strong, moderate, and very weak bleaching or lack of bleaching is very similar; thus, only the x-ray patterns for selected horizons are presented (Fig. 2). The x-ray patterns show that the clay fraction is composed mainly of 2:1 clay minerals exhibiting a $\sim 1.4 \text{ nm}$ peak in air dry state. The peak does not fully collapse to 1.0 nm neither after the heating of the samples at $330 \text{ }^\circ\text{C}$ nor $550 \text{ }^\circ\text{C}$ (Fig. 2). However, it should be noted that the collapse of the ~ 1.4 to 1.0 nm peak is much stronger after the heating of specimens at $550 \text{ }^\circ\text{C}$. Treatment with glycerol also does not affect the $\sim 1.4 \text{ nm}$ peak (Fig. 2). Kaolinite ($\sim 0.7 \text{ nm}$ peak

Table 3 Physical and chemical properties of the soils

Horizon	Depth (cm)	Sand (%)	Silt	Clay	Db ^a (Mg m ⁻³)	P ^b (%)	pH H ₂ O	Corg (%)	Fe _d ^c g kg ⁻¹	Fe _o ^d	Al _o ^e
Plešna 1											
O	0–2	N.A.	N.A.	N.A.	N.A.	N.A.	N.A.	N.A.	N.A.	N.A.	N.A.
A	2–10	17	68	15	1.18	53.7	4.2	1.2	4.91	2.6	0.9
AE	10–30	17	70	13	1.31	49.2	5.1	0.5	5.23	2.6	0.5
E	30–70	18	69	13	1.32	49.2	5.2	0.3	4.94	2.7	0.6
Btx	70–105	15	67	18	1.42	45.8	4.9	0.1	7.56	2.9	0.7
Btg	105–150	14	67	19	1.42	46.0	5.0	0.1	7.30	2.4	0.6
BC	150–200	21	66	13	1.40	47.2	5.3	0.1	6.57	1.5	0.3
Plešna 2											
A	0–10	13	71	16	1.50	42.3	5.0	0.7	5.65	3.2	0.8
AE	10–30	15	73	12	1.44	45.0	5.2	0.5	4.36	2.6	0.6
E	30–55	13	74	13	1.58	39.5	5.5	0.3	4.92	3.2	0.8
Btx1	55–80	11	71	18	1.65	36.5	5.6	0.1	7.29	3.6	0.8
Btx2	80–160	11	70	19	1.66	36.2	5.4	0.1	7.09	2.4	0.5
Plešna 3											
Ap	0–35	14	72	14	1.54	40.3	5.1	0.8	4.78	3.9	1.3
Eg	35–45	12	73	15	1.57	40.1	5.6	0.4	9.02	4.8	1.4
Btx1	45–100	13	68	19	1.63	38.0	6.0	0.1	7.73	6.0	1.5
Btx2	100–180	10	72	18	1.62	37.7	5.4	0.1	7.91	4.0	1.1
Btg	180–245	13	69	18	1.61	38.8	5.2	0.1	4.84	2.9	1.1
BCg	245–285	11	73	16	N.A.	N.A.	5.7	0.1	7.01	3.5	1.1
Plešna 4											
O	0–2	N.A.	N.A.	N.A.	N.A.	N.A.	4.3	N.A.	N.A.	N.A.	N.A.
A	2–10	21	66	13	N.A.	N.A.	4.1	3.8	4.46	2.9	0.9
E	10–40	13	74	13	1.26	52.6	4.2	0.4	4.22	2.9	0.8
Eg	40–90	13	74	13	1.58	40.8	4.3	0.1	4.23	3.2	0.7
Btx	90–150	9	66	25	1.63	39.6	5.2	0.1	6.65	2.6	0.6
Łazy 1											
Ap	0–35	21	71	8	1.27	51.2	6.4	0.9	4.26	2.5	1.4
Eg	35–50	21	68	11	1.53	43.1	6.7	0.2	5.21	2.9	1.2
Btx	50–70	15	62	23	1.61	39.7	6.1	0.2	10.72	2.8	1.7
Btg	70–90	18	65	17	1.56	42.4	5.5	0.1	7.61	2.7	1.4
BC	90–110	16	71	13	1.56	41.8	5.7	0.1	5.92	2.9	1.1
C	110–150	18	69	13	1.65	38.7	5.6	0.1	4.35	2.7	1.0
Łazy 2											
Ol	0–5	N.A.	N.A.	N.A.	N.A.	N.A.	4.2	N.A.	N.A.	N.A.	N.A.
Of	5–8	N.A.	N.A.	N.A.	N.A.	N.A.	4.5	N.A.	N.A.	N.A.	N.A.
A	8–20	23	64	13	0.80	68.3	3.9	3.0	5.67	3.2	0.9
E	20–55	11	78	11	1.30	50.8	4.2	0.4	5.05	2.6	0.8
Btx1	55–65	18	63	19	1.44	46.3	4.0	0.3	8.33	2.5	1.2
Btx2	65–85	18	63	19	1.60	39.8	4.7	0.2	8.94	1.8	1.0
Bt	85–115	20	64	16	1.60	40.7	5.0	0.2	7.33	1.8	0.6
BC	115–135	21	64	15	1.55	42.8	4.9	0.1	7.15	1.6	0.5
C	135–185	22	65	13	1.57	41.4	5.0	0.1	7.58	1.5	0.5
Łazy 3											
Ol	0–3	N.A.	N.A.	N.A.	N.A.	N.A.	N.A.	N.A.	N.A.	N.A.	N.A.
A	3–11	18	70	12	1.19	54.6	6.6	1.1	5.54	2.5	0.9
AE	11–25	20	67	13	1.33	49.0	6.5	0.7	5.4	1.2	0.9
Eg	25–50	20	68	12	1.44	45.2	6.3	0.5	5.65	1.3	1.4
Bh	50–70	19	70	11	1.31	50.6	6.0	0.8	4.82	1.2	1.5
Btx1	70–110	16	66	18	1.66	38.5	5.3	0.2	7.45	1.1	0.9
Btx2	110–160	20	65	15	N.A.	N.A.	5.3	0.1	6.5	0.9	0.6
Łazy 4											
Ol	0–2	N.A.	N.A.	N.A.	N.A.	N.A.	N.A.	N.A.	N.A.	N.A.	N.A.
Ah	2–5	21	68	11	N.A.	N.A.	4.3	6.1	5.61	1.2	0.9
E	5–20	19	69	12	1.40	47.2	4.4	0.6	4.48	1.1	0.7
Eg	20–35	21	68	11	1.48	42.6	4.6	0.4	4.31	1.1	0.5
Btx1	35–60	16	70	14	1.55	41.5	5.5	0.2	5.96	1.1	0.6
Btx2	60–85	14	63	23	1.59	41.5	5.3	0.1	10.3	0.9	0.6
Btg	85–140	19	64	17	1.56	41.4	5.4	0.1	7.05	0.8	0.5
BCg	140–180	19	67	14	1.58	39.9	5.3	0.1	6.22	0.7	0.4
Grabie											
Ol	0–2	N.A.	N.A.	N.A.	N.A.	N.A.	N.A.	N.A.	N.A.	N.A.	N.A.
Ofh	2–4	N.A.	N.A.	N.A.	N.A.	N.A.	4.2	N.A.	N.A.	N.A.	N.A.

Table 3 (continued)

Horizon	Depth (cm)	Sand (%)	Silt	Clay	Db ^a (Mg m ⁻³)	P ^b (%)	pH H ₂ O	Corg (%)	Fe _d ^c g kg ⁻¹	Fe _o ^d	Al _o ^e
Ah	4–12	14	73	13	N.A.	N.A.	4.2	3.6	5.66	2.7	1.4
Eg	12–35	13	72	15	1.33	50.0	4.4	0.4	5.58	2.5	1.3
Btx1	35–70	12	64	24	1.58	40.6	5.0	0.1	9.41	2.5	1.3
Btx2	70–120	19	61	20	1.63	39.6	5.0	0.1	8.73	2.6	0.9
Btx3	120–155	10	69	21	1.66	39.0	5.1	0.1	8.48	1.7	0.7
2C	155–165	6	56	38	N.A.	N.A.	5.9	0.2	N.A.	N.A.	N.A.
Radziszów											
Of	0–2	N.A.	N.A.	N.A.	N.A.	N.A.	5.0	N.A.	N.A.	N.A.	N.A.
Ah	2–12	18	69	13	N.A.	N.A.	4.3	3.6	5.4	3.1	1.4
E	12–35	13	77	10	1.21	54.0	4.5	0.3	5.27	2.9	1.3
Eg	35–45	12	79	9	1.41	47.2	4.5	0.2	4.62	2.2	0.9
Btx1	45–75	11	68	21	1.57	41.9	5.0	0.1	8.59	2.3	1.3
Btx2	75–100	12	70	18	1.63	40.3	5.2	0.1	8.63	2.7	1.1
Btx3	100–120	15	53	32	1.78	35.0	5.5	0.1	13.31	2.2	1.0
BC	120–130	28	32	40	1.71	37.4	5.6	0.2	17.83	2.6	0.9
2C	130–160	27	34	39	N.A.	N.A.	7.9	0.2	N.A.	N.A.	N.A.
Polanka Hallera											
Ap	0–20	13	74	13	1.40	46.7	6.9	1.2	5.3	1.1	0.5
A	20–37	11	76	11	1.53	39.4	7.3	0.8	5.57	1.2	0.7
Eg	37–50	12	79	8	1.60	38.5	7.5	0.2	5.61	1.0	0.4
Btx	50–60	12	69	19	1.65	35.7	7.5	0.1	8.44	1.0	0.8
Btg1	60–85	10	70	19	1.65	43.1	7.4	0.1	8.69	0.9	0.7
Btg2	85–120	12	69	19	1.67	33.9	5.6	0.1	6.51	0.7	0.4
Btg3	120–155	10	74	16	1.73	35.0	6.0	0.1	5.13	0.8	0.4
Btg4	155–180	10	70	19	N.A.	N.A.	6.7	0.1	10.98	1.0	0.4
Brzezcie											
Ap	0–25	14	71	15	1.55	40.8	5.3	1.1	5.32	3.7	N.A.
AE1	25–40	10	75	15	1.50	43.8	5.4	0.7	5.65	4.2	N.A.
AE2	40–58	9	76	15	1.45	45.3	5.4	0.7	5.62	4.3	N.A.
Eg	58–70	16	74	10	1.41	46.6	5.4	0.2	3.73	3.3	N.A.
Btx	70–95	11	67	22	1.68	37.5	5.1	0.1	8.50	3.8	N.A.
Btg1	95–115	10	69	21	1.67	38.1	5.4	0.1	7.50	2.0	N.A.
Btg2	115–180	16	68	16	1.70	36.3	6.0	0.1	5.62	1.5	N.A.

^a Bulk density^b Total porosity^c CBD extractable Fe^d AAO-extractable Fe^e AAO-extractable Al

N.A. not analyzed

disappeared after heating at 550 °C), mica (~1.0, 0.5 nm peaks not affected by the various tests), and quartz (~0.43 nm peak) are also present (Fig. 2). XRD results obtained for the clay fractions clearly indicate that the intensity of bleaching (strong vs. moderate or weak or lack), being a result of different duration and frequency of periodic water stagnation and redox processes above a hard and slowly permeable fragipan in the soils, does not affect the quality of clay minerals found in the Retisols of the Carpathian Foothills.

Quantitative mineral composition of the eluvial horizons (fraction <2 mm) is presented in Table 5, and selected x-ray patterns presenting the bulk mineral composition are presented in Fig. 3. All of the eluvial horizons (E and Eg) are characterized by a predominance of quartz. Quartz content ranges from 60 to 72 %. The mean quartz content in the E and Eg horizons is 69 and 67 %, respectively. K-feldspar content

ranges from 9 to 11 % with a mean content of 10 % in the E and Eg horizons. Plagioclase content is slightly lower than K-feldspar content and ranges from 6 to 9 %. Mean plagioclase content in the E and Eg horizons is almost the same, i.e., 8 and 7 %, respectively. Dioctahedral mica found in the eluvial horizons (E and Eg) range between 3 and 5 % with a mean content of 4 % in the E and Eg horizons. Chlorite and kaolinite content in eluvial horizons is very low: 0–2 % chlorite, 1–2 % kaolinite. Mean chlorite content is 1 % and mean kaolinite content is 2 % in the E and Eg horizons of interest. The content of interlayered 2:1 clay minerals is between 4 and 8 %. The E and Eg horizons contain almost equal mean concentrations of the interlayered 2:1 clay minerals, i.e., 7 and 6 %, respectively. The results of both the qualitative analysis of clay fraction and the quantitative analysis of the bulk mineral composition of the eluvial horizons indicate a lack of significant differences at

Table 4 Chemical composition of the soils

Horizon	Depth (cm)	SiO ₂ (%)	Al ₂ O ₃ (%)	Fe ₂ O ₃ (%)	MgO (%)	CaO (%)	Na ₂ O (%)	K ₂ O (%)	TiO ₂ (%)	P ₂ O ₅ (%)	MnO (%)	Other (%)
Plešna 1												
O	0–2	N.A.	N.A.	N.A.	N.A.	N.A.	N.A.	N.A.	N.A.	N.A.	N.A.	N.A.
A	2–10	80.37	7.58	2.14	0.47	0.31	0.98	1.88	0.69	0.09	0.04	5.45
AE	10–30	81.34	7.81	2.17	0.50	0.40	1.01	1.98	0.73	0.09	0.06	3.91
E	30–70	82.35	7.49	1.96	0.47	0.37	0.97	1.91	0.71	0.08	0.07	3.62
Btx	70–105	77.94	9.40	3.18	0.74	0.44	0.94	2.13	0.71	0.08	0.06	4.38
Btg	105–150	78.47	9.25	3.09	0.73	0.45	0.93	2.16	0.68	0.10	0.06	4.08
BC	150–200	79.05	9.07	2.90	0.74	0.54	1.19	2.21	0.71	0.11	0.07	3.41
Plešna 2												
A	0–10	79.06	8.19	2.48	0.55	0.35	0.87	2.14	0.73	0.10	0.08	5.45
AE	10–30	82.67	7.35	1.90	0.43	0.35	0.91	2.06	0.76	0.10	0.09	3.38
E	30–55	81.47	7.80	1.99	0.46	0.38	0.90	2.14	0.77	0.09	0.12	3.88
Btx1	55–80	77.95	9.48	3.11	0.73	0.42	0.83	2.29	0.73	0.08	0.06	4.32
Btx2	80–160	78.38	9.48	3.07	0.73	0.44	0.93	2.32	0.72	0.09	0.07	3.77
Plešna 3												
Ap	0–35	80.62	7.68	2.24	0.47	0.40	0.87	2.07	0.76	0.16	0.10	4.63
Eg	35–45	80.80	8.03	2.32	0.50	0.42	0.88	2.14	0.75	0.13	0.10	3.93
Btx1	45–100	77.35	9.52	3.27	0.73	0.51	0.83	2.32	0.73	0.11	0.07	4.56
Btx2	100–180	78.07	9.43	3.15	0.74	0.50	0.92	2.38	0.72	0.12	0.05	3.92
Btg	180–245	79.34	9.14	2.60	0.70	0.51	0.95	2.29	0.72	0.10	0.06	3.59
BCg	245–285	78.72	9.35	3.00	0.72	0.55	1.01	2.36	0.73	0.12	0.07	3.37
Plešna 4												
O	0–2	N.A.	N.A.	N.A.	N.A.	N.A.	N.A.	N.A.	N.A.	N.A.	N.A.	N.A.
A	2–10	77.38	6.61	1.57	0.32	0.30	0.88	1.83	0.69	0.10	0.02	10.30
E	10–40	82.73	7.37	1.81	0.40	0.31	0.98	2.07	0.76	0.05	0.06	3.46
Eg	40–90	82.91	7.60	1.88	0.43	0.33	0.99	2.11	0.76	0.10	0.09	2.80
Btx	90–150	77.57	9.60	3.26	0.77	0.49	0.93	2.32	0.72	0.10	0.06	4.18
Łazy 1												
Ap	0–35	83.12	6.38	1.67	0.38	0.55	0.85	1.93	0.66	0.20	0.07	4.19
Eg	35–50	83.49	7.15	2.00	0.46	0.44	0.92	2.03	0.68	0.07	0.06	2.70
Btx	50–70	79.34	8.75	3.09	0.68	0.48	0.83	2.08	0.65	0.07	0.05	3.98
Btg	70–90	79.85	8.51	3.17	0.64	0.43	0.84	2.06	0.66	0.07	0.05	3.72
BC	90–110	81.35	7.93	2.63	0.58	0.43	0.82	1.99	0.65	0.08	0.05	3.49
C	110–150	82.40	7.65	2.25	0.56	0.40	0.85	1.98	0.62	0.07	0.05	3.17
Łazy 2												
Ol	0–5	N.A.	N.A.	N.A.	N.A.	N.A.	N.A.	N.A.	N.A.	N.A.	N.A.	N.A.
Of	5–8	N.A.	N.A.	N.A.	N.A.	N.A.	N.A.	N.A.	N.A.	N.A.	N.A.	N.A.
A	8–20	N.A.	N.A.	N.A.	N.A.	N.A.	N.A.	N.A.	N.A.	N.A.	N.A.	N.A.
E	20–55	83.75	6.12	1.70	0.34	0.25	0.79	1.71	0.64	0.08	0.04	4.58
Btx1	55–65	80.41	8.04	2.77	0.59	0.23	0.76	1.87	0.64	0.08	0.05	4.56
Btx2	65–85	79.20	8.70	3.20	0.68	0.35	0.78	1.92	0.64	0.10	0.05	4.38
Bt	85–115	80.66	8.18	2.78	0.63	0.39	0.81	1.92	0.63	0.09	0.05	3.86
BC	115–135	82.16	7.66	2.49	0.56	0.40	0.83	1.86	0.62	0.07	0.05	3.30
C	135–185	82.01	7.54	2.61	0.55	0.40	0.86	1.90	0.60	0.08	0.06	3.39
Łazy 3												
Ol	0–3	N.A.	N.A.	N.A.	N.A.	N.A.	N.A.	N.A.	N.A.	N.A.	N.A.	N.A.
A	3–11	81.56	6.79	1.87	0.43	0.51	0.79	1.88	0.66	0.18	0.07	5.26
AE	11–25	83.50	6.53	1.74	0.39	0.44	0.78	1.81	0.67	0.14	0.08	3.92
Eg	25–50	82.89	6.94	1.79	0.38	0.40	0.79	1.96	0.69	0.16	0.11	3.89
Bh	50–70	83.43	6.72	1.61	0.38	0.37	0.81	1.98	0.67	0.12	0.07	3.84
Btx1	70–110	80.18	8.28	2.83	0.63	0.37	0.73	1.98	0.66	0.11	0.05	4.18
Btx2	110–160	82.09	7.54	2.48	0.57	0.37	0.80	1.93	0.62	0.07	0.04	3.49
Łazy 4												
Ol	0–2	N.A.	N.A.	N.A.	N.A.	N.A.	N.A.	N.A.	N.A.	N.A.	N.A.	N.A.
Ah	2–5	71.41	6.06	2.05	0.35	0.39	0.72	1.63	0.62	0.15	0.04	16.58
E	5–20	84.19	6.45	1.53	0.35	0.29	0.89	1.94	0.68	0.08	0.05	3.55
Eg	20–35	84.59	6.48	1.51	0.34	0.29	0.89	1.95	0.70	0.08	0.07	3.10
Btx1	35–60	82.21	7.76	2.23	0.55	0.36	0.94	2.17	0.72	0.09	0.06	2.91
Btx2	60–85	77.66	9.21	3.65	0.76	0.41	0.81	2.11	0.69	0.06	0.05	4.59
Btg	85–140	80.51	8.44	2.77	0.64	0.40	0.90	2.07	0.65	0.07	0.06	3.49
BCg	140–180	81.57	7.96	2.41	0.58	0.41	0.94	2.14	0.67	0.06	0.06	3.20
Grabie												
Ol	0–2	N.A.	N.A.	N.A.	N.A.	N.A.	N.A.	N.A.	N.A.	N.A.	N.A.	N.A.
Ofh	2–4	N.A.	N.A.	N.A.	N.A.	N.A.	N.A.	N.A.	N.A.	N.A.	N.A.	N.A.
Ah	4–12	77.57	6.35	1.73	0.34	0.29	0.68	1.87	0.66	0.11	0.03	10.37

Table 4 (continued)

Horizon	Depth (cm)	SiO ₂ (%)	Al ₂ O ₃ (%)	Fe ₂ O ₃ (%)	MgO (%)	CaO (%)	Na ₂ O (%)	K ₂ O (%)	TiO ₂ (%)	P ₂ O ₅ (%)	MnO (%)	Other (%)
Eg	12–35	82.20	7.76	2.06	0.46	0.33	0.82	2.34	0.75	0.12	0.07	3.09
Btx1	35–70	77.19	9.66	3.43	0.68	0.37	0.77	2.32	0.72	0.12	0.04	4.70
Btx2	70–120	76.81	9.78	3.33	0.73	0.46	0.87	2.44	0.73	0.10	0.05	4.70
Btx3	120–155	76.05	10.36	3.42	0.86	0.58	1.04	2.53	0.76	0.10	0.06	4.24
2C	155–165	62.95	15.59	5.86	2.31	0.77	1.21	3.10	0.73	0.16	0.11	7.21
Radziszów												
Of	0–2	N.A.	N.A.	N.A.	N.A.	N.A.	N.A.	N.A.	N.A.	N.A.	N.A.	N.A.
Ah	2–12	77.50	6.55	1.67	0.32	0.33	0.73	1.98	0.69	0.08	0.03	10.12
E	12–35	83.23	7.22	1.73	0.37	0.31	0.79	2.17	0.74	0.05	0.05	3.34
Eg	35–45	84.13	7.06	1.63	0.38	0.33	0.85	2.28	0.74	0.04	0.04	2.52
Btx1	45–75	78.32	9.47	3.18	0.64	0.35	0.78	2.34	0.72	0.06	0.04	4.10
Btx2	75–100	76.97	9.84	3.44	0.69	0.44	0.86	2.33	0.75	0.07	0.04	4.57
Btx3	100–120	71.86	11.92	4.53	1.04	0.59	0.71	2.52	0.75	0.07	0.05	5.96
BC	120–130	67.23	12.98	5.61	1.34	0.68	0.50	2.58	0.68	0.10	0.08	8.22
2C	130–160	65.62	12.37	4.77	1.32	3.10	0.45	2.56	0.63	0.23	0.05	8.90
Polanka Hallera												
Ap	0–20	79.73	6.93	2.07	0.39	0.71	0.78	2.07	0.71	0.19	0.07	6.36
A	20–37	80.69	6.96	2.05	0.39	0.71	0.80	2.07	0.73	0.15	0.07	5.40
Eg	37–50	84.16	7.23	1.94	0.42	0.49	0.89	2.29	0.77	0.08	0.04	1.70
Btx	50–60	79.04	8.98	3.09	0.61	0.57	0.80	2.29	0.77	0.08	0.08	3.70
Btg1	60–85	77.86	9.33	3.25	0.50	0.56	0.83	2.29	0.75	0.05	0.05	4.54
Btg2	85–120	79.00	8.57	3.21	0.57	0.51	0.87	2.23	0.72	0.06	0.07	4.24
Btg3	120–155	79.73	9.24	2.74	0.64	0.55	0.98	2.38	0.75	0.06	0.05	2.90
Btg4	155–180	N.A.	N.A.	N.A.	N.A.	N.A.	N.A.	N.A.	N.A.	N.A.	N.A.	N.A.
Brzezie												
Ap	0–25	80.00	7.65	2.23	0.46	0.47	0.79	1.99	0.66	0.15	0.06	5.54
AE1	25–40	80.22	7.82	2.28	0.47	0.46	0.78	2.02	0.68	0.13	0.06	5.08
AE2	40–58	80.65	7.81	2.16	0.46	0.43	0.76	2.01	0.68	0.12	0.05	4.87
Eg	58–70	84.77	6.68	1.53	0.36	0.35	0.79	2.03	0.67	0.06	0.07	2.69
Btx	70–95	78.63	9.05	3.15	0.64	0.42	0.74	2.14	0.69	0.06	0.05	4.43
Btg1	95–115	79.91	8.62	2.91	0.60	0.45	0.80	2.14	0.66	0.05	0.04	3.82
Btg2	115–180	81.05	8.10	2.46	0.55	0.53	0.90	2.16	0.67	0.07	0.04	3.47

^a Loss on ignition

N.A. not analyzed

$p < 0.05$ (t Student test) between E and Eg horizons in the Retisols. This is most likely due to the fact that the Retisols of the Carpathian Foothills contain very little iron-bearing minerals.

3.2.2 FTIR spectroscopy

Analysis of FTIR spectra obtained for the clay fractions (<2 μm) separated from eluvial horizons supports the earlier interpretation of XRD data. Due to the fact that all of the obtained FTIR spectra are almost identical, only spectra for selected eluvial horizons are presented (Fig. 4). Assignments for the major FTIR bands are presented in Table 6. Two strong absorption bands at ~ 3699 and ~ 3620 cm^{-1} are present in the OH stretching region and indicate presence of kaolinite and dioctahedral 2:1 clay minerals (Table 6). All weak absorption bands in the OH stretching region are related to vibrations of Al–OH–Al in the structure of kaolinite and/or dioctahedral mica (Table 6, Fig. 5) (Besson and Drits 1997; Madejová

2003; Zviagina et al. 2004). Strong absorption bands present at ~ 1165 , 1085, 799, and 780 cm^{-1} in the Si–O and OH bending regions are related to quartz and silicates (Table 6, Fig. 4). In addition, two broad bands at ~ 1620 and ~ 1405 cm^{-1} are present and originate from organic matter (Table 6) (Celi et al. 1997; Coccozza et al. 2003; Tivet et al. 2013) and water, because the bands become weaker after heating at 180 °C and disappear almost completely after treatment with hydrogen peroxide (see Szymański et al. 2014). The presence of ~ 2926 and ~ 2855 cm^{-1} bands is associated with methyl and methylene groups, respectively (Ellerbrock and Gerke 2004), while the wide band at ~ 3430 cm^{-1} indicates H–O–H vibrations of structurally adsorbed water molecules (Table 6) (Bain and Fraser 1994; Besson and Drits 1997; Madejová 2003). The FTIR data also indicate the lack of discernible water stagnation effects and redox effects on the different transformation pathways of clay minerals in strongly, moderately, and weakly bleached eluvial horizons as well as in eluvial horizons without bleaching.

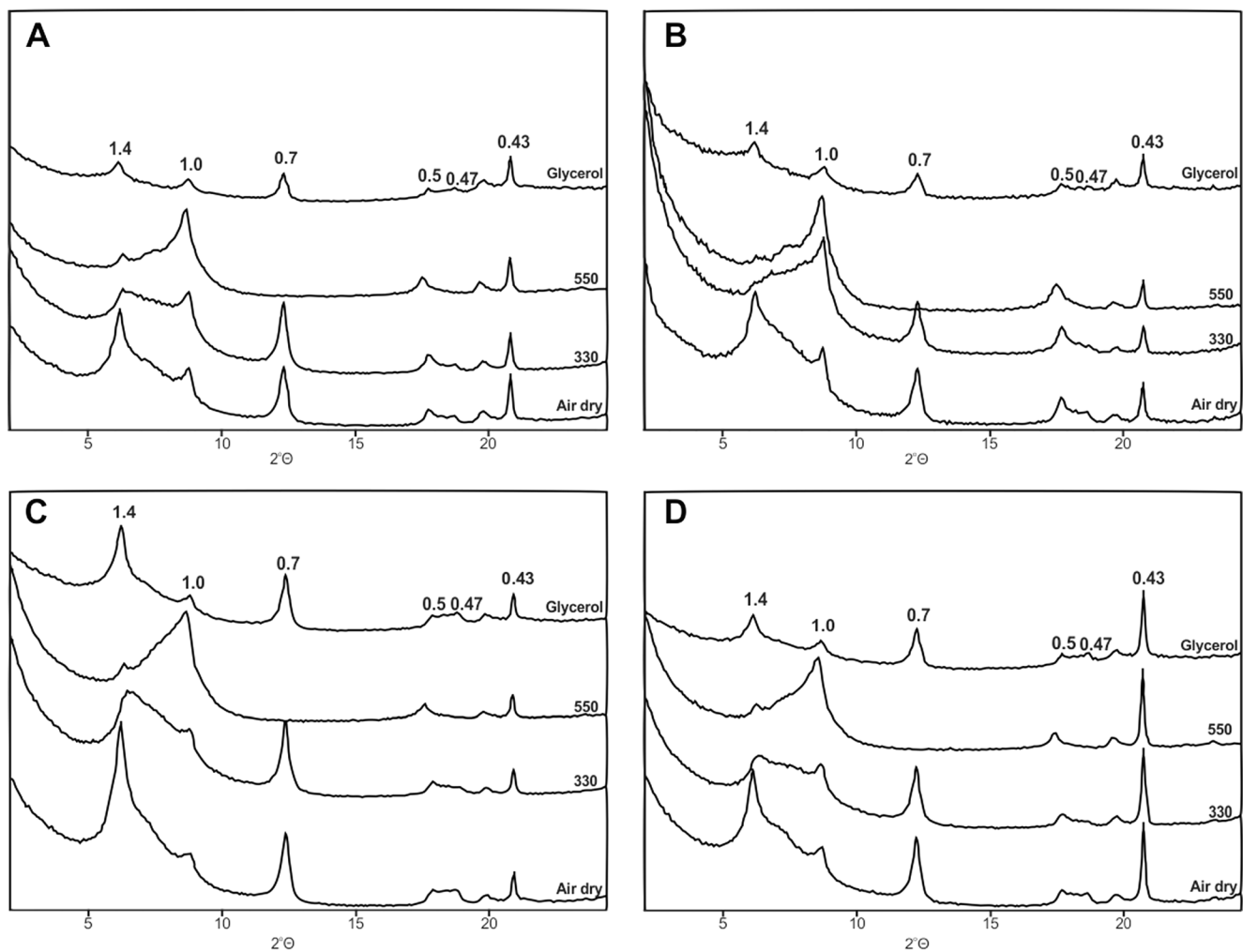
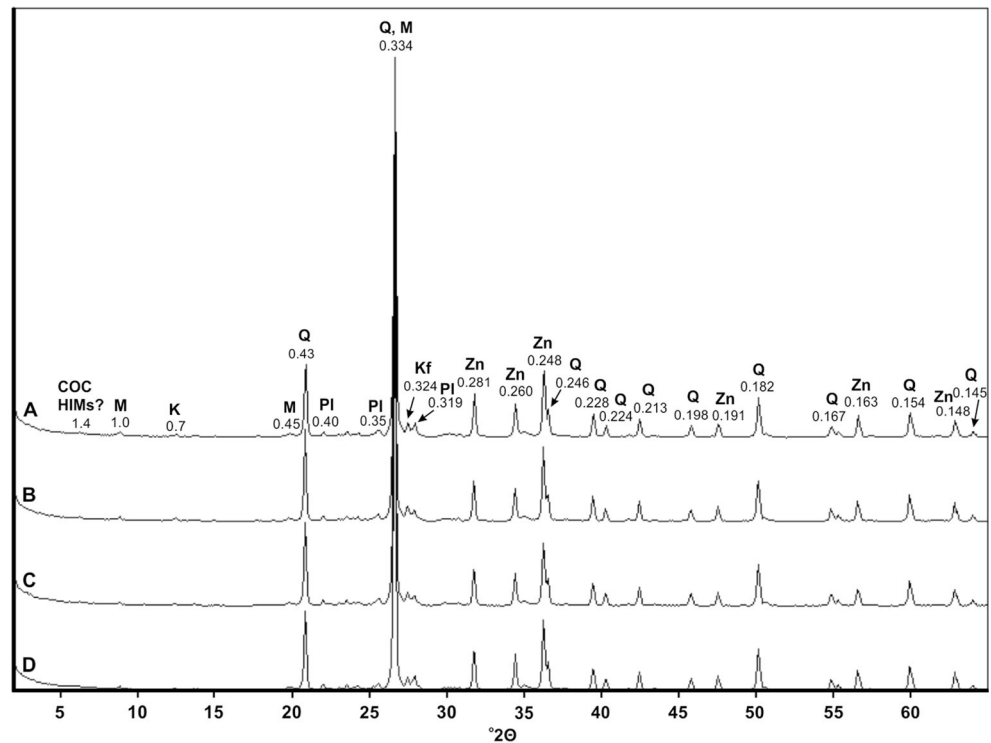


Fig. 2 XRD patterns of the clay fraction (<2 μm) from selected eluvial horizons: Eg horizon of the Brzezie profile (a); E horizon of the Pleśna 1 profile (b); E horizon of the Radziszów profile (c); Eg horizon of the Radziszów profile (d)

Table 5 Quantitative mineral composition of bulk samples (< 2 mm) of the E and Eg horizons

Profile and horizon	Quartz (%)	K-feldspars (%)	Plagioclases (%)	Diocahedral micas (%)	Chlorite (%)	Kaolinite (%)	Interlayered 2:1 clay minerals (%)	Amorphous (%)
Pleśna 1 E	68	9	9	4	1	2	6	1
Pleśna 2 E	67	10	8	4	2	1	7	1
Pleśna 3 Eg	60	9	8	4	1	2	6	10
Pleśna 4 E	70	10	9	3	0	1	6	1
Pleśna 4 Eg	69	10	9	4	0	2	5	1
Łazy 1 Eg	63	9	7	4	1	2	7	7
Łazy 2 E	69	9	7	4	2	2	7	0
Łazy 3 Eg	69	9	6	5	0	2	6	3
Łazy 4 E	70	10	8	3	1	1	7	0
Łazy 4 Eg	71	10	8	4	0	2	5	0
Grabie Eg	64	11	7	5	2	1	6	4
Radziszów E	69	11	7	3	0	2	8	0
Radziszów Eg	71	10	7	4	2	2	4	0
Polanka Hallera Eg	67	11	8	4	1	2	6	1
Brzezie Eg	68	9	7	3	1	1	6	5

Fig. 3 XRD patterns of bulk samples (<2 mm) of the selected eluvial horizons from: Eg horizon of the Polanka Hallera profile (a); Eg horizon of the Radziszów profile (b); E horizon of the Radziszów profile (c); E horizon of the Pleśna 1 profile (d)



3.2.3 Mössbauer spectroscopy

Mössbauer spectroscopy results obtained for the clay fractions are shown in Table 7, and selected Mössbauer spectra are shown in Fig. 6. The data indicate that the relative content of Fe³⁺ and Fe²⁺ is not related to the intensity of bleaching of eluvial horizons within the same soil profile and between different profiles. In case of Łazy 4 and Radziszów profiles,

relative Fe²⁺ content is higher in the Eg horizons than in the E horizons while in Pleśna 4 profile, the relative content of Fe²⁺ is lower in the Eg horizon than in the E horizon. The same is true for E and Eg horizons originating from different soil profiles—the relative content of Fe²⁺ is higher in the Eg horizons from the Pleśna 3 profile than in the E horizon from the Pleśna 1 profile, but at the same time, it is lower than the relative content of Fe²⁺ in the E horizon from the Pleśna 4

Fig. 4 FTIR spectra of the clay fraction (<2 μm) from selected eluvial horizons: Eg horizon of the Brzezie profile (a); E horizon of the Pleśna 1 profile (b); E horizon of the Radziszów profile (c); Eg horizon of the Radziszów profile (d)

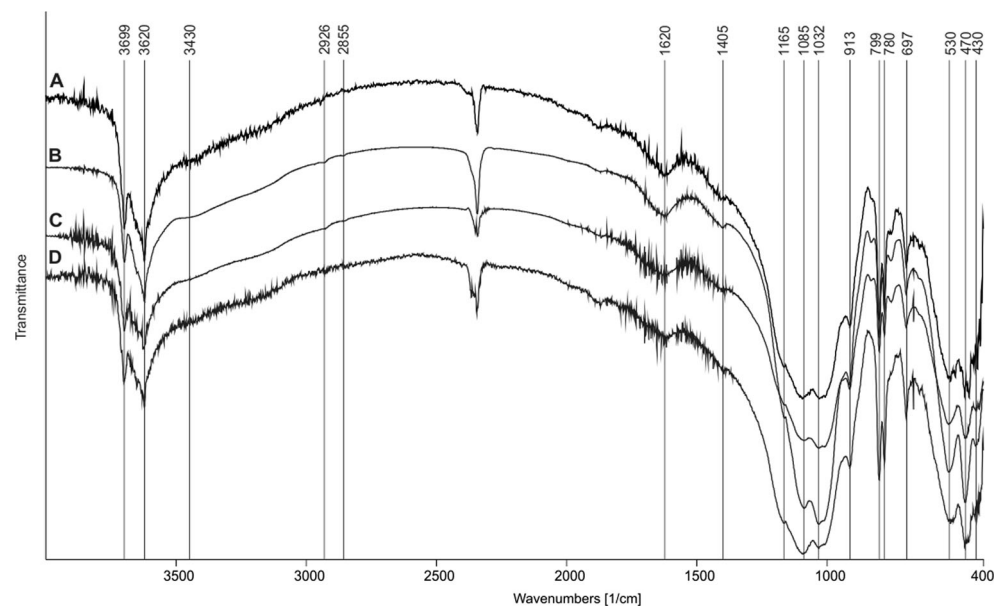


Table 6 Assignments for the major FTIR bands

FTIR peak position	Assignment
cm ⁻¹	
3699	Al–OH–Al of kaolinite
3620	Al–OH–Al of kaolinite and/or dioctahedral 2:1 clay minerals
3655	Al–OH–Al of kaolinite and/or dioctahedral 2:1 clay minerals
3687	Al–OH–Al of kaolinite and/or dioctahedral 2:1 clay minerals
3674	Al–OH–Al of kaolinite and/or dioctahedral 2:1 clay minerals
3646	Al–OH–Al of kaolinite and/or dioctahedral 2:1 clay minerals
3633	Al–OH–Al of kaolinite and/or dioctahedral 2:1 clay minerals
3626	Al–OH–Al of kaolinite and/or dioctahedral 2:1 clay minerals
3430	H–O–H of water molecules
2926	C–H of methyl groups
2855	C–H of methylene groups
1620	aromatic C=C and C=O of carboxylic acid
1405	aliphatic C–H and C–OH deformation of COOH groups
1165	Si–O stretching of quartz and silicates
1085	Si–O stretching of quartz and silicates
799	Si–O stretching of quartz and silicates
780	Si–O stretching of quartz and silicates

profile (Table 7). The mean relative content of Fe²⁺ in the clay fraction in the Eg horizons is only slightly higher (7.7 %) than the mean for the clay fraction obtained from E horizons (7.6 %). These results also indicate a lack of relationship between water stagnation and redox processes and relative content of iron in different oxidation states in the clay fraction of the eluvial horizons (E and Eg).

3.3 Verification of ferrollysis occurrence in Retisols

The Retisols with Eg horizons showing strong bleaching (Pleśna 3, Pleśna 4, Łazy 1, Polanka Hallera, and Brzezcie profiles) are very similar to the ferrollyzed soils studied by Brinkman (1979). They are characterized by a strongly bleached, coarser-grained horizon underlain by mottled, finer-grained horizons with bleached vertical tongues (Szymański et al. 2011). In addition, the bleached horizons contain a large number of Fe–Mn nodules indicating redox processes, and all of the soils are characterized by acidic or slightly acidic pH, with the exception of the Polanka Hallera profile. The strongly bleached Eg horizons of the Retisols exhibit the occurrence of clay minerals with interlayering characterized by a lack of complete collapse after heating as well as a lack of discernible swelling after glycerol solvation (Fig. 2). All the above-mentioned characteristics may indicate that ferrollysis occurs in these soils. However, the same clay minerals featuring interlayering were also identified in other Eg horizons with moderate or very weak bleaching as well as in E horizons, which do not exhibit bleaching at all and contain either few or no Fe–Mn nodules indicating very weak or a

lack of redox processes. Thus, the obtained research results indicate the lack of a clear influence of redox processes (due to

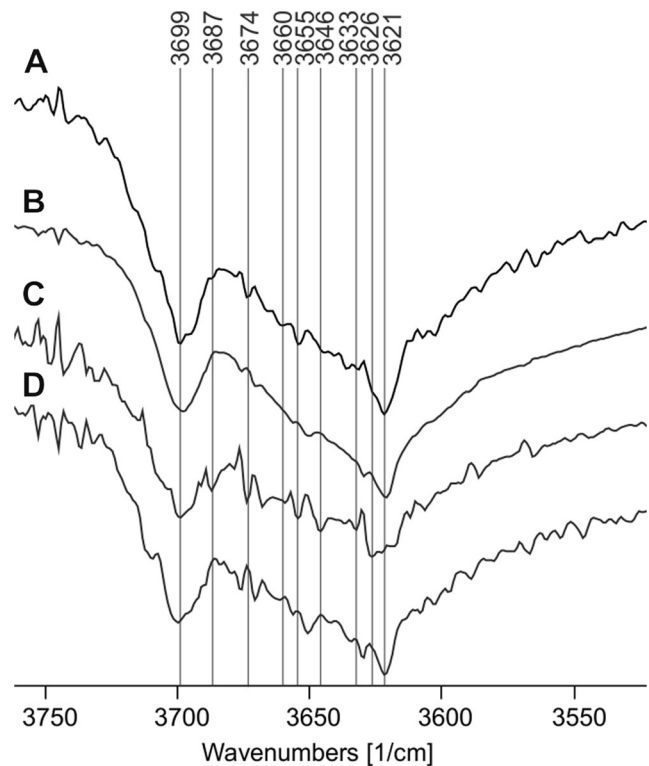


Fig. 5 FTIR spectra of the clay fraction (<2 μm) in the OH stretching region from selected eluvial horizons: Eg horizon of the Brzezcie profile (a); E horizon of the Pleśna 1 profile (b); E horizon of the Radziszów profile (c); Eg horizon of the Radziszów profile (d)

Table 7 Relative content of Fe²⁺ and Fe³⁺ in crystalline structure of clay fraction (<0.002 mm) in the E and Eg horizons

Horizon	Iron valence state	A ^a (%) ±0.2	IS ^b (mm/s) ±0.01	QS ^c (mm/s) ±0.01
Pleśna 1	E Fe ³⁺	95.0	0.38	0.65
	Fe ²⁺	5.0	1.10	2.66
Pleśna 2	E Fe ³⁺	91.9	0.36	0.71
	Fe ²⁺	8.1	1.12	2.48
Pleśna 3	Eg Fe ³⁺	94.0	0.38	0.66
	Fe ²⁺	6.0	1.11	2.63
Pleśna 4	E Fe ³⁺	91.7	0.37	0.71
	Fe ²⁺	8.3	1.12	2.58
	Eg Fe ³⁺	93.0	0.36	0.71
	Fe ²⁺	7.0	1.12	2.49
Łazy 1	Eg Fe ³⁺	90.6	0.37	0.74
	Fe ²⁺	9.4	1.13	2.50
Łazy 2	E Fe ³⁺	91.6	0.37	0.73
	Fe ²⁺	8.4	1.15	2.49
Łazy 3	Eg Fe ³⁺	92.2	0.36	0.73
	Fe ²⁺	7.8	1.12	2.44
Łazy 4	E Fe ³⁺	91.1	0.36	0.74
	Fe ²⁺	8.9	1.12	2.47
	Eg Fe ³⁺	90.0	0.37	0.74
	Fe ²⁺	10.0	1.13	2.47
Grabie	Eg Fe ³⁺	93.1	0.36	0.72
	Fe ²⁺	6.9	1.14	2.49
Radziszów	E Fe ³⁺	92.9	0.35	0.71
	Fe ²⁺	7.1	1.10	2.47
	Eg Fe ³⁺	91.6	0.35	0.70
	Fe ²⁺	8.4	1.10	2.51
Polanka Hallera	Eg Fe ³⁺	94.9	0.35	0.70
	Fe ²⁺	5.1	1.11	2.43
Brzezie	Eg Fe ³⁺	91.1	0.36	0.72
	Fe ²⁺	8.9	1.12	2.58

^a Contribution of the respective sub-profile to the total absorption profile equivalent to content of Fe³⁺ and Fe²⁺

^b Isomer shift.

^c Quadrupole splitting

periodic stagnation of water above the slowly permeable fragipan) on clay mineral transformation in the Retisols. In addition, a prior study (Szymański et al. 2014) indicates that clay minerals in the E and Eg horizons of the soils contain mainly organic fillings in their interlayers and not metal-hydroxy polymers, as indicated by Brinkman (1979). The neoformation of fine quartz in bleached horizons, proposed by Brinkman (1977, 1979) and Brinkman et al. (1973) as a secondary product of weathering due to ferrollysis was not observed in the Retisols, because the presence of quartz in the clay fraction was observed in both E and Eg horizons (Fig. 2), and also in other horizons of the soils (Szymański et al. 2011, 2014). In addition, if the ferrollysis leads to the neoformation of fine quartz, and if the process does occur in the Eg horizons, then, the Eg horizons should contain a clearly higher amount of quartz than the E horizons. However, precisely the opposite outcome (i.e., slightly higher mean content of quartz in E versus Eg horizons but not statistically significant at *p* < 0.05) was identified in the Retisols (Table 5). In addition, the mean chlorite content is the same (Table 5) in the

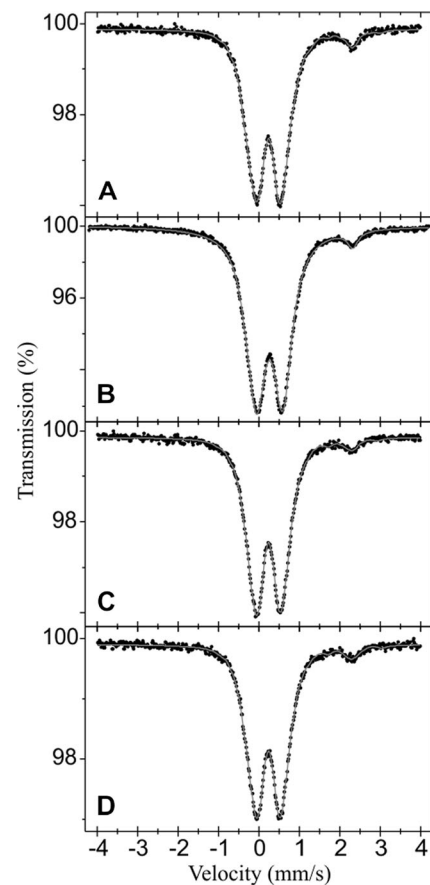


Fig. 6 Mössbauer spectra of the clay fraction (<2 μm) from selected eluvial horizons: Eg horizon of the Brzezie profile (a); E horizon of the Pleśna 1 profile (b); E horizon of the Radziszów profile (c); Eg horizon of the Radziszów profile (d)

E and Eg horizons, but according to Brinkman (1979), the chlorite content should be higher in ferrolyzed horizons in comparison with other horizons. The results of our study are in agreement with Van Ranst and De Coninck (2002) and Van Ranst et al. (2011) who assert that ferrolysis is not the main soil-forming process in bleached soils as in Retisols (Albeluvisols) and Planosols, and it is not responsible for texture contrasts in these soils.

4 Conclusions

The obtained results indicate that the qualitative and quantitative mineral compositions of the clay fraction in the E and Eg horizons obtained from Retisols in the Carpathian Foothills in Poland exhibiting marked differences in bleaching (strong, moderate, weak, and lack of bleaching) caused by periodic stagnation of water above a slowly permeable fragipan and cyclic redox processes are the same. The E and Eg horizons are characterized by the presence of 2:1 clay minerals with likely organic interlayer fillings, dioctahedral mica, kaolinite, and chlorite. These findings indicate that (1) redox processes occurring in the soils do not affect clay mineral transformation and (2) ferrolysis is not the main soil-forming process operating in these soils. This is most likely because iron-bearing minerals are not abundant in Retisols of the Carpathian Foothills and/or undergo eluviation to the lower part of the soil profiles. The lower content of the clay fraction in the E and Eg horizons versus that in the lower soil horizons of the Retisols is related to clay illuviation (*lessivage*), and not to clay decomposition due to ferrolysis.

Acknowledgments This study was financed by Poland's National Science Centre based on Decision Number DEC-2012/05/D/ST10/00527. The authors would like to thank Adam Michalski from the Department of Pedology at the Nicolaus Copernicus University in Toruń for providing iron and aluminum oxides laboratory data. The authors would like to thank the Editor and anonymous reviewers for helpful suggestions. Language editing was done by Grzegorz Zębik.

Open Access This article is distributed under the terms of the Creative Commons Attribution 4.0 International License (<http://creativecommons.org/licenses/by/4.0/>), which permits unrestricted use, distribution, and reproduction in any medium, provided you give appropriate credit to the original author(s) and the source, provide a link to the Creative Commons license, and indicate if changes were made.

References

- Bain DC, Fraser AR (1994) An unusually interlayered clay mineral from the eluvial horizon of a humus-iron podzol. *Clay Miner* 29:69–76
- Barbiero L, Mohan Kumar MS, Violette A, Oliva P, Braun JJ, Kumar C, Furian S, Babic M, Riotte J, Valles V (2010) Ferrolysis induced soil transformation by natural drainage in Vertisols of sub-humid South India. *Geoderma* 156:173–188
- Besson G, Drits VA (1997) Refined relationships between chemical composition of dioctahedral fine-grained mica minerals and their infrared spectra within the OH stretching region. Part I: identification of the OH stretching bands. *Clay Clay Miner* 45:158–169
- Boivin P, Saejiew A, Grunberger O, Arunin S (2004) Formation of soils with contrasting textures by translocation of clays rather than ferrolysis in flooded rice fields in Northeast Thailand. *Eur J Soil Sci* 55:713–724
- Brinkman R (1970) Ferrolysis, a hydromorphic soil forming process. *Geoderma* 3(3):199–206
- Brinkman R (1977) Surface-water gley soils in Bangladesh: genesis. *Geoderma* 17(2):111–144
- Brinkman R (1979) Ferrolysis, a soil-forming process in hydromorphic conditions. Doctoral thesis. Agricultural Research Reports 887, Centre for Agricultural Publishing and Documentation, Wageningen
- Brinkman R, Jongmans AG, Miedema R, Maaskant P (1973) Clay decomposition in seasonally wet, acid soils: micromorphological, chemical and mineralogical evidence from individual argillans. *Geoderma* 10(4):259–270
- Celi L, Schnitzer M, Negre M (1997) Analysis of carboxyl groups in soil humic acids by a wet chemical method, Fourier-transform infrared spectrophotometry, and solution-state carbon-13 nuclear magnetic resonance. A comparative study. *Soil Sci* 162(3):189–197
- Cescas MP, Tyner EH, Harmer IIRS (1970) Ferromanganiferous soil concretions: a scanning electron microscope study of their micro-pore structures. *Soil Sci Soc Am J* 34:641–644
- Ciolkosz EJ, Waltman WJ, Thurman NC (1995) Fragipans in Pennsylvania soils. *Soil survey. Horizons* 36:5–20
- Cocozza C, D'Orazio V, Miano TM, Shotyk W (2003) Characterization of solid and aqueous phases of a peat bog profile using molecular fluorescence spectroscopy, ESR and FT-IR, and comparison with physical properties. *Organic Geochem* 34(1):49–60
- Dixon JB, White GN (2002) Manganese oxides. In: Dixon JB, Schulze DG (eds) *Soil mineralogy with environmental applications*. SSSA Book Ser. 7. Soil Science Society of America Inc., Madison, WI, USA. pp 367–388
- Drewnik M, Skiba M, Szymański W, Żyła M (2014) Mineral composition vs. soil forming processes in loess soils—a case study from Kraków (southern Poland). *Catena* 119:166–173
- Ellerbrock RH, Gerke HH (2004) Characterizing organic matter of soil aggregate coatings and biopores by Fourier transform infrared spectroscopy. *Eur J Soil Sci* 55(2):219–228
- Gee GW, Bauder JW (1986) Particle-size analysis. In: Klute A (ed), *Methods of soil analysis*. Part 1. Physical and mineralogical methods, 2nd edition. Agronomy Monograph. vol. 9. ASA-SSSA, Madison, Wisconsin, pp 427–445
- Gerstl Z, Banin A (1980) Fe²⁺-Fe³⁺ transformations in clay and resin ion-exchange systems. *Clay Clay Miner* 28(5):335–345
- Hardy M, Jamagne M, Elsass F, Robert M, Chesneau D (1999) Mineralogical development of the silt fractions of a Podzoluvisol on loess in the Paris Basin (France). *Eur J Soil Sci* 50:443–456
- Hess M (1965) Altitudinal climatic zones in the Polish Western Carpathians. *Zeszyty. Naukowe UJ Prace Geograficzne* 11 (in Polish)
- Hobson WA, Dahlgren RA (1998) Soil forming processes in vernal pools of Northern California, Chico Area. In: Witham CW, Bauder ET, Belk D, Ferren Jr. WR, Ornduff R (eds) *Ecology, conservation, and management of vernal pool ecosystems—proceedings from a 1996 conference*. California Native Plant Society, Sacramento, CA, pp 24–37
- IUSS Working Group WRB (2014) World reference base for soil resources 2014. World Soil Resources Reports No. 106. FAO, Rome
- Jackson ML (1969) *Soil chemical analysis—advance course*, 2nd edn. University of Wisconsin, Madison, WI
- Kalinina O, Chertov O, Dolgikh AV, Goryachkin SV, Lyuri DI, Vormstein S, Giani L (2013) Self-restoration of post-agrogenic Albeluvisols:

- soil development, carbon stocks and dynamics of carbon pools. *Geoderma* 207–208:221–233
- Kemp RA, McIntosh PD (1989) Genesis of a texturally-banded soil in Southland, New Zealand. *Geoderma* 85:65–81
- Klimaszewski M (1967) The polish western Carpathians in quaternary period. In: Galon R, Dylik J (eds) . *Quaternary of Poland*, PWN, Warszawa, pp. 431–497 in Polish
- Kohut C, Warren CJ (2002) Chlorite. In: Dixon JB, Schulze DG (eds) *Soil mineralogy with environmental applications*. Soil Sci. Soc. Am, Madison, WI, pp. 531–556
- Leigh DS (1998) Evaluating artifact burial by eolian versus bioturbation processes, South Carolina Sandhills, USA. *Geoarchaeology* 13: 309–330
- Lindbo DL, Veneman PLM (1993) Micromorphology of selected Massachusetts fragipan soils. *Soil Sci Soc Am J* 57:437–442
- Lindbo DL, Rhoton FE, Bigham JM, Hudnall WH, Jones FS, Smeck NE, Tyler DD (1994) Bulk density and fragipan identification in loess soils of the lower Mississippi River valley. *Soil Sci Soc Am J* 58: 884–891
- Lindbo DL, Rhoton FE, Bigham JM, Hudnall WH, Jones FS, Smeck NE, Tyler DD (1995) Loess toposequences in the lower Mississippi River valley: I. Fragipan morphology and identification. *Soil Sci Soc Am J* 59:487–500
- Lindbo DL, Rhoton FE, Hudnall WH, Smeck NE, Bigham JM, Tyler DD (2000) Fragipan degradation and nodule formation in Glossic Fragiudalfs of the lower Mississippi River valley. *Soil Sci Soc Am J* 64:1713–1722
- Madejová J (2003) FTIR techniques in clay mineral studies. *Vib Spectrosc* 31:1–10
- Montagne D, Cornu S, Le Forestier L, Hardy M, Josière O, Caner L, Cousin I (2008) Impact of drainage on soil-forming mechanisms in a French Albeluvisol: input of mineralogical data in mass-balance modelling. *Geoderma* 145:426–438
- Moore D, Reynolds RC (1997) *X-ray diffraction and the identification and analysis of clay minerals*. Oxford University Press, Oxford
- Mystkowski K (1999) ClayLab, a computer program for processing and interpretation of x-ray diffractograms of clays. Conference of European Clay Groups Association, EUROCLAY 1999, Book of Abstracts, Kraków, Poland, pp 114–115
- Nakao A, Funakawa S, Kosaki T (2009) Hydroxy-Al polymers block the frayed edge sites of illitic minerals in acid soils: studies in southwestern Japan at various weathering stages. *Eur J Soil Sci* 60:127–138
- Nelson DW, Sommers LE (1996) Total carbon, organic carbon, and organic matter. In: Sparks DL, Page AL, Helmke PA et al. (eds) *Methods of soil analysis. Part 3. Chemical methods SSSA Book Series. vol. 5. SSSA and ASA, Madison, Wisconsin*, pp 961–1010
- Nikorych VA, Szymański W, Polchyna SM, Skiba M (2014) Genesis and evolution of the fragipan in Albeluvisols in the Precarpathians in Ukraine. *Catena* 119:154–165
- Peacock E, Fant DW (2002) Biomantle formation and artifact translocation in upland sandy soils, an example from the Holly Springs National Forest, north-central Mississippi, U.S.A. *Geoarchaeology* 17:91–114
- Phillips JD (2001) Contingency and generalization in pedology, as exemplified by texture-contrast soils. *Geoderma* 102:347–370
- Phillips JD (2004) Geogenesis, pedogenesis, and multiple causality in the formation of texture-contrast soils. *Catena* 58:275–295
- Phillips JD (2007) Development of texture contrast soils by a combination of bioturbation and translocation. *Catena* 70:92–104
- Rhoton FE, Bigham JM, Schulze DG (1993) Properties of iron-manganese nodules from a sequence of eroded fragipan soils. *Soil Sci Soc Am J* 57:1386–1392
- Rich CI (1968) Hydroxy interlayers in expansible layer silicates. *Clay Clay Miner* 16:15–30
- Rozenon I, Heller-Kallai L (1978) Reduction and oxidation of Fe³⁺ in dioctahedral smectites—III. Oxidation of octahedral iron in montmorillonite. *Clay Clay Miner* 26(2):88–92
- Sauer D, Schüllli-Maurer I, Sperstad R, Sørensen R (2013) Micromorphological characteristics reflecting soil-forming processes during Albeluvisol development in S Norway. *Spanish. J Soil Sci* 3(2):38–58
- Schlichting E, Blume HP (1966) *Bodenkundliches Praktikum*. Verlag Paul Parey, Hamburg-Berlin
- Schwertmann U, Fanning DS (1976) Iron-manganese concretions in hydrosequences of soils in loess in Bavaria. *Soil Sci Soc Am J* 40: 731–738
- Skiba S, Drewnik M (2003) Soil map of the polish Carpathians. *Roczniki Bieszczadzkie* 11:15–20 in Polish
- Środoń J (2006) Identification and quantitative analysis of clay minerals. In: Bergaya F et al. (eds) *Handbook of clay science*. Elsevier, Amsterdam, pp. 765–787
- Starkel L (1972) The Outer Carpathians. In: Klimaszewski M (ed) *Geomorphology of Poland, Southern Poland, mountains and uplands*, PWN, Warszawa, pp 55–115 (in Polish)
- Świtoniak M (2008) Classification of young glacial soils with vertical texture-contrast using WRB system. *Agrochimija i Gruntoznawstwo* 69:96–101
- Świtoniak M (2014) Use of soil profile truncation to estimate influence of accelerated erosion on soil cover transformation in young morainic landscapes, north-eastern Poland. *Catena* 116:173–184
- Świtoniak M, Mroczek P, Bednarek R (2016) Luvisols or Cambisols? Micromorphological study of soil truncation in young morainic landscapes—case study: Brodnica and Chełmno Lake districts (North Poland). *Catena* 137:583–595
- Szymański W, Skiba M (2013) Distribution, morphology, and chemical composition of Fe-Mn nodules in Albeluvisols of the Carpathian foothills, Poland. *Pedosphere* 23(4):445–454
- Szymański W, Skiba M, Skiba S (2011) Fragipan horizon degradation and bleached tongues formation in Albeluvisols of the Carpathian Foothills, Poland. *Geoderma* 167–168:340–350
- Szymański W, Skiba M, Skiba S (2012) Origin of reversible cementation and brittleness of the fragipan horizon in Albeluvisols of the Carpathian foothills, Poland. *Catena* 99:66–74
- Szymański W, Skiba M, Nikorych VA, Kuligiewicz A (2014) Nature and formation of interlayer fillings in clay minerals in Albeluvisols from the Carpathian foothills, Poland. *Geoderma*:235–236 396–409
- Taut T, Kleeberg R, Bergmann J (1998) The new Seifert Rietveld program BGMN and its application to quantitative phase analysis. *Materials Structure* 5(1):57–64
- Thomas GW (1996) Soil pH and soil acidity. In: Sparks DL, Page AL, Helmke PA, Loeppert RH (eds) *Methods of soil analysis. Part 3. Chemical methods SSSA book series, 5 edn. SSSA and ASA, Madison, Wisconsin*, pp. 475–490
- Tivet F, Sá JCM, Lal R, Milori DMBP, Briedis C, Letourmy P, Pinheiro LA, Borszowskei PR, Hartman DC (2013) Assessing humification and organic C compounds by laser-induced fluorescence and FTIR spectroscopies under conventional and no-till management in Brazilian Oxisols. *Geoderma* 207–208:71–81
- Towpaz K, Zemanek B (1995) Vegetation. In: Warszńska J (ed), *Polish Carpathian Mts.—Environment, Man, and His Activity*. Wyd. UJ, Kraków, pp 77–94 (in Polish)
- Van Ranst E, De Coninck F (2002) Evaluation of ferrollysis in soil formation. *Eur J Soil Sci* 53:513–519
- Van Ranst E, Dumon M, Tolossa AR, Cornelis JT, Stoops G, Vandenberghe RE, Deckers J (2011) Revisiting ferrollysis processes in the formation of Planosols for rationalizing the soils with stagnic properties in WRB. *Geoderma* 163:265–274
- Van Reeuwijk LP (2002) *Procedures for soil analysis*, 6th edn. ISRIC, Wageningen

- Weisenborn BN, Schaetzl RJ (2005) Range of fragipan expression in some Michigan soils: I. Morphological, micromorphological, and pedogenic characterization. *Soil Sci Soc Am J* 69:168–177
- Witty JE, Knox EG (1989) Identification, role in soil taxonomy and worldwide distribution of fragipans. In: Smeck NE, Ciolkosz EJ (eds) *Fragipans: their occurrence, classification and genesis*. SSSA Spec. Publ., 24. SSSA, Madison, Wisconsin, pp 1–9
- Zasoński S (1983) Main soil-forming processes on loess-like deposits of the Wieliczka foothills. Part II. Micromorphological properties. *Roczniki Gleboznawcze* 34(4):123–161 in Polish
- Zasoński S (1992) Micromorphological properties of silty soils of the Krosno Valley. *Zeszyty Naukowe AR* 265:19–33 in Polish
- Zhang M, Karathanasis AD (1997) Characterization of iron-manganese concretions in Kentucky Alfisols with perched water tables. *Clay Clay Miner* 45:428–439
- Zviagina BB, McCarty DK, Środoń J, Drits VA (2004) Interpretation of infrared spectra of dioctahedral smectites in the region of OH-stretching vibrations. *Clay Clay Miner* 52: 399–410